# Photon bandwidth dependence of light-matter interaction

MATTHIAS STEINER,[1,2] VICTOR LEONG,[1,2,3] MATHIAS ALEXANDER SEIDLER,[1] ALESSANDRO CERÈ,[1] AND CHRISTIAN KURTSIEFER[1,2,*]

[1] *Center for Quantum Technologies, 3 Science Drive 2, Singapore 117543*
[2] *Department of Physics, National University of Singapore, 2 Science Drive 3, Singapore 117542*
[3] *Present address: Data Storage Institute, Agency for Science, Technology and Research (A*STAR), Singapore 138634, Singapore*
[*] *christian.kurtsiefer@gmail.com*

**Abstract:** We investigate the scattering of single photons by single atoms and, in particular, the dependence of the atomic dynamics and the scattering probability on the photon bandwidth. We tightly focus the incident photons onto a single trapped $^{87}$Rb atom and use the time-resolved transmission to characterize the interaction strength. Decreasing the bandwidth of the single photons from 6 to 2 times the atomic linewidth, we observe an increase in atomic peak excitation and photon scattering probability.



**OCIS codes:** (020.0020) Atomic and molecular physics; (270.0270) Quantum optics; (300.2570) Four-wave mixing.

## References and links

1. Z.-L. Xiang, S. Ashhab, J. Q. You, and F. Nori, "Hybrid quantum circuits: Superconducting circuits interacting with other quantum systems," Rev. Mod. Phys. **85**, 623–653 (2013).
2. G. Kurizki, P. Bertet, Y. Kubo, K. Molmer, D. Petrosyan, P. Rabl, and J. Schmiedmayer, "Quantum technologies with hybrid systems," PNAS **112**, 3866–3873 (2015).
3. H. J. Kimble, "The quantum internet," Nature **453**, 1023–1030 (2008).
4. E. Waks and C. Monroe, "Protocol for hybrid entanglement between a trapped atom and a quantum dot," Phys. Rev. A **80**, 062330 (2009).
5. T. Wilk, S. C. Webster, A. Kuhn, and G. Rempe, "Single-atom single-photon quantum interface," Science **317**, 488–490 (2007).
6. S. Ritter, C. Nolleke, C. Hahn, A. Reiserer, A. Neuzner, M. Uphoff, M. Mucke, E. Figueroa, J. Bochmann, and G. Rempe, "An elementary quantum network of single atoms in optical cavities," Nature **484**, 195–200 (2012).
7. N. Akopian, L. Wang, A. Rastelli, O. G. Schmidt, and V. Zwiller, "Hybrid semiconductor-atomic interface: slowing down single photons from a quantum dot," Nat. Photon. **5**, 230–233 (2011).
8. S. M. Ulrich, S. Weiler, M. Oster, M. Jetter, A. Urvoy, R. Löw, and P. Michler, "Spectroscopy of the $D_1$ transition of cesium by dressed-state resonance fluorescence from a single (in,ga)as/gaas quantum dot," Phys. Rev. B **90**, 125310 (2014).
9. P. Siyushev, G. Stein, J. Wrachtrup, and I. Gerhardt, "Molecular photons interfaced with alkali atoms," Nature **509**, 66–70 (2014).
10. J.-P. Jahn, M. Munsch, L. Béguin, A. V. Kuhlmann, M. Renggli, Y. Huo, F. Ding, R. Trotta, M. Reindl, O. G. Schmidt, A. Rastelli, P. Treutlein, and R. J. Warburton, "An artificial rb atom in a semiconductor with lifetime-limited linewidth," Phys. Rev. B **92**, 245439 (2015).
11. H. M. Meyer, R. Stockill, M. Steiner, C. Le Gall, C. Matthiesen, E. Clarke, A. Ludwig, J. Reichel, M. Atatüre, and M. Köhl, "Direct photonic coupling of a semiconductor quantum dot and a trapped ion," Phys. Rev. Lett. **114**, 123001 (2015).
12. G. Leuchs and M. Sondermann, "Light-matter interaction in free space," Journal of Modern Optics **60**, 36–42 (2013).
13. V. Leong, M. A. Seidler, M. Steiner, A. Cerè, and C. Kurtsiefer, "Time-resolved scattering of a single photon by a single atom," Nat. Commun. **7**, 13716 (2016).
14. V. Bužek, G. Drobný, M. G. Kim, M. Havukainen, and P. L. Knight, "Numerical simulations of atomic decay in cavities and material media," Phys. Rev. A **60**, 582–592 (1999).
15. S. J. van Enk and H. J. Kimble, "Single atom in free space as a quantum aperture," Phys. Rev. A **61**, 051802 (2000).
16. S. J. van Enk and H. J. Kimble, "Strongly focused light beams interacting with single atoms in free space," Phys. Rev. A **63**, 023809 (2001).
17. S. J. van Enk, "Atoms, dipole waves, and strongly focused light beams," Phys. Rev. A **69**, 043813 (2004).

18. P. Domokos, P. Horak, and H. Ritsch, "Quantum description of light-pulse scattering on a single atom in waveguides," Phys. Rev. A **65**, 033832 (2002).
19. D. Pinotsi and A. Imamoglu, "Single photon absorption by a single quantum emitter," Phys. Rev. Lett. **100**, 093603 (2008).
20. G. Zumofen, N. M. Mojarad, V. Sandoghdar, and M. Agio, "Perfect reflection of light by an oscillating dipole," Phys. Rev. Lett. **101**, 180404 (2008).
21. G. Wrigge, I. Gerhardt, J. Hwang, G. Zumofen, and V. Sandoghdar, "Efficient coupling of photons to a single molecule and the observation of its resonance fluorescence," Nat. Phys. **4**, 60–66 (2008).
22. S. Heugel, A. S. Villar, M. Sondermann, U. Peschel, and G. Leuchs, "On the analogy between a single atom and an optical resonator," Laser Physics **20**, 100–106 (2009).
23. M. Stobińska, G. Alber, and G. Leuchs, "Perfect excitation of a matter qubit by a single photon in free space," EPL **86**, 14007 (2009).
24. M. K. Tey, G. Maslennikov, T. C. H. Liew, S. A. Aljunid, F. Huber, B. Chng, Z. Chen, V. Scarani, and C. Kurtsiefer, "Interfacing light and single atoms with a lens," New J. Phys. **11**, 043011 (2009).
25. Y. Wang, J. Minář, L. Sheridan, and V. Scarani, "Efficient excitation of a two-level atom by a single photon in a propagating mode," Phys. Rev. A **83**, 063482 (2011).
26. G. Leuchs and M. Sondermann, "Time-reversal symmetry in optics," Physica Scripta **85**, 058101 (2012).
27. N. Trautmann, G. Alber, and G. Leuchs, "Efficient single-photon absorption by a trapped moving atom," Phys. Rev. A **94**, 033832 (2016).
28. V. Weisskopf and E. Wigner, "Berechnung der natürlichen linienbreite auf grund der diracschen lichttheorie," Zeitschr. Phys. **63**, 54–73 (1930).
29. T. Chanelière, D. N. Matsukevich, and S. D. Jenkins, "Quantum telecommunication based on atomic cascade transitions," Phys. Rev. Lett. **96**, 093604 (2006).
30. B. Srivathsan, G. K. Gulati, B. Chng, G. Maslennikov, D. Matsukevich, and C. Kurtsiefer, "Narrow band source of transform-limited photon pairs via four-wave mixing in a cold atomic ensemble," Phys. Rev. Lett. **111**, 123602 (2013).
31. J. Brito, S. Kucera, P. Eich, P. Müller, and J. Eschner, "Doubly heralded single-photon absorption by a single atom," Appl. Phys. B **122**, 1–5 (2016).
32. M. K. Tey, Z. Chen, S. A. Aljunid, B. Chng, F. Huber, G. Maslennikov, and C. Kurtsiefer, "Strong interaction between light and a single trapped atom without the need for a cavity," Nat. Phys. **4**, 924–927 (2008).
33. J. D. Franson, "Nonlocal cancellation of dispersion," Phys. Rev. A **45**, 3126–3132 (1992).
34. B. Srivathsan, G. K. Gulati, A. Cerè, B. Chng, and C. Kurtsiefer, "Reversing the temporal envelope of a heralded single photon using a cavity," Phys. Rev. Lett. **113**, 163601 (2014).
35. G. K. Gulati, B. Srivathsan, B. Chng, A. Cerè, D. Matsukevich, and C. Kurtsiefer, "Generation of an exponentially rising single-photon field from parametric conversion in atoms," Phys. Rev. A **90**, 033819 (2014).
36. H. H. Jen, "Spectral analysis for cascade-emission-based quantum communication in atomic ensembles," J. Phys. B: At. Mol. Opt. Phys. **45**, 165504 (2012).
37. Y.-S. Chin, M. Steiner, and C. Kurtsiefer, "Quantifying the role of thermal motion in free-space light-atom interaction," arXiv:1611.08048 [quant-ph] (2016).
38. N. P. Georgiades, E. S. Polzik, K. Edamatsu, H. J. Kimble, and A. S. Parkins, "Nonclassical excitation for atoms in a squeezed vacuum," Phys. Rev. Lett. **75**, 3426–3429 (1995).
39. M. Strauß, M. Placke, S. Kreinberg, C. Schneider, M. Kamp, S. Höfling, J. Wolters, and S. Reitzenstein, "Photon-statistics excitation spectroscopy of a single two-level system," Phys. Rev. B **93**, 241306 (2016).
40. L. Alber, M. Fischer, M. Bader, K. Mantel, M. Sondermann, and G. Leuchs, "Focusing characteristics of a $4\pi$ parabolic mirror light-matter interface," arXiv:1609.06884 [quant-ph] (2016).

## 1. Introduction

Hybrid quantum systems aim to overcome difficulties in implementing more complex quantum information processing tasks with individual quantum systems [1, 2] - a quantum network with solid-state systems as fast processors, atomic systems as long-lived memories, and optical photons interfacing spatially separated network nodes is an example [3, 4]. There, control over the spectral and temporal properties of the exchanged photons is desirable for efficient information transfer [5, 6], but can be hard or impractical to implement. A common problem in hybrid quantum networks is a mismatch between the characteristic time scale (or bandwidth) of photons emitted by one node with the optical transition of the receiving node [7–11]. Understanding the role of the photon bandwidth in light-matter interaction is therefore important for the further development of hybrid networks.

One realization of an atomic node of a quantum network is a single atom in free space coupled to a strongly focused mode [12]. Aside from the potential use in quantum networks, single atoms

are also an ideal test bed to study fundamental properties of light-matter interaction. Following up on recent work on time-resolved scattering of photons with exponentially rising and decaying profiles [13], we report in this work on the dependency of single photon scattering on the photon bandwidth.

## 2. Theory

The interaction between single atoms and light has been studied extensively in semi-classical and fully quantized frameworks [14–27]. Interesting recent results were the complete reflection of light by a single atom [20, 24], and the complete absorption of a single photon by reversing the spontaneous emission process from an excited two-level atom into spherical harmonic modes [19, 23, 25, 28].

Practically important cases for traveling photons with a finite duration have an exponential temporal envelope, and consequently a Lorentzian power spectrum

$$\mathcal{L}(\omega) \propto \frac{1}{(\omega-\omega_0)^2 + \Gamma_\mathrm{p}^2/4} \tag{1}$$

of width $\Gamma_\mathrm{p}$ centered at the atomic resonance frequency $\omega_0$. For a single photon Fock state with Lorentzian power spectrum [Eq. (1)], the scattering probability $\epsilon$ is obtained by solving Eq. 18 and Eq. 21 in [25],

$$\epsilon = 4\Lambda(1-\Lambda)\frac{\Gamma_0}{\Gamma_0+\Gamma_\mathrm{p}}, \tag{2}$$

where $\Gamma_0$ is the width of the atomic line of interest and $\Lambda \in [0,1]$ is the spatial overlap between the excitation and the atomic dipole mode [12, 13]. Here, the scattering probability $\epsilon$ is the probability to scatter the incident photon into a spatial mode different from the excitation mode. In the absorption experiment presented in Sec. 3, we determine $\epsilon$ by detecting the photons in excitation mode after passing the atom. The scattering probability $\epsilon$ is then equal to the *extinction*, i.e. the reduction of detected photons due to the interaction with the atom.

Photons of different temporal envelopes can have identical power spectra – for example, both exponentially rising and falling temporal envelopes lead to a Lorentzian power spectrum. In the work presented here, we consider an exponential decaying envelope $P_\mathrm{p}(t)$ for the photon in the time domain,

$$P_\mathrm{p}(t) = \Gamma_\mathrm{p}\Theta(t)\exp\left(-\Gamma_\mathrm{p}t\right), \tag{3}$$

where $\Theta(t)$ is the Heaviside step function. For such a photon the probability $P_\mathrm{e}(t)$ of finding a two-level atom in the excited state is given by [13, 23]

$$P_\mathrm{e}(t) = \frac{4\Lambda\Gamma_0\Gamma_\mathrm{p}}{(\Gamma_0-\Gamma_\mathrm{p})^2}\Theta(t)\left[\exp\left(-\frac{1}{2}\Gamma_0 t\right) - \exp\left(-\frac{1}{2}\Gamma_\mathrm{p}t\right)\right]^2, \tag{4}$$

with an atomic peak excitation probability

$$P_\mathrm{e,max} = 4\Lambda\left(\frac{\Gamma_\mathrm{p}}{\Gamma_0}\right)^{\frac{\Gamma_0+\Gamma_\mathrm{p}}{\Gamma_0-\Gamma_\mathrm{p}}}. \tag{5}$$

According to this model, the highest atomic peak excitation probability is reached if the bandwidth of the incident photon matches the atomic linewidth, $\Gamma_\mathrm{p} = \Gamma_0$, while the highest scattering probability is obtained for very narrowband excitation, $\Gamma_\mathrm{p} \to 0$ [Eq. (2)].

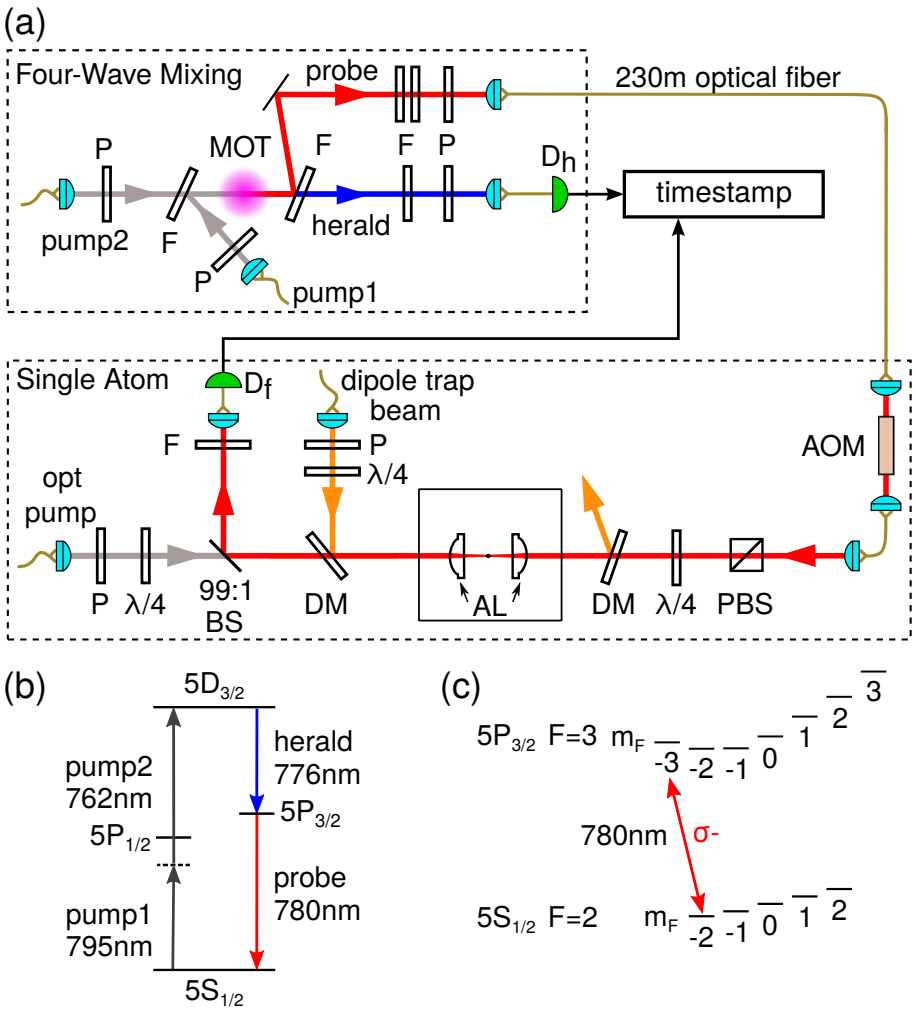


Fig. 1. **(a)** Optical setup to prepare heralded single photons at 780 nm which are tightly focused on a single trapped atom. Four-wave mixing: two co-aligned pump fields (pump1 at 795 nm and pump2 at 762 nm) generate herald (776 nm) and probe (780 nm) photon pairs in a cold cloud of $^{87}$Rb atoms. The detection of a herald photon at $D_h$ signals the presence of a single photon in the probe mode. Single Atom: a $^{87}$Rb atom is trapped at the focus of a confocal aspheric lens pair (AL) with an optical dipole trap. $D_h$, $D_f$: avalanche photodetectors, P: polarizer, F: interference filter, $\lambda/2$, $\lambda/4$: half- and quarter-wave plate, (P)BS: (polarizing) beam splitter, DM: dichroic mirror, AOM: acousto-optic modulator, MOT: magneto-optical trap. **(b)** Level scheme of the FWM process. **(c)** Level scheme of the single $^{87}$Rb atom in the dipole trap.

## 3. Experiment

To test the model presented in Sec. 2, we prepare single photon states by heralding on a time-correlated photon-pair from a parametric process in a cold atomic ensemble [29, 30]. These photons are focused onto a single atom trapped in a far-off-resonant optical dipole trap. From the fraction of photons that are scattered out of this focused excitation mode, we can accurately obtain the transient atomic excitation [13, 31]

The experimental setup is shown in Fig. 1(a). A single atom is loaded from a cold ensemble

in a magneto-optical trap (MOT) into a far-off-resonant optical dipole trap [32] formed by the tight focus of a light beam prepared by an aspheric lens (numerical aperture 0.55). The dipole trap laser (980 nm, 42 mW, circular polarization) provides a trap depth of approximately 2 mK. Once trapped, the atom undergoes molasses cooling and is optically pumped into the $5S_{1/2}$, $F$=2, $m_F$=-2 state. A bias magnetic field of 0.7 mT is applied along the optical axis.

We obtain heralded single photons from correlated photon pairs generated by four-wave-mixing (FWM) in a cloud of cold $^{87}$Rb atoms. This atomic cloud is repeatedly cooled and refilled by a MOT for 140 $\mu$s, followed by a photon pair generation interval of 10 $\mu$s. During the photon pair generation, two pump beams with wavelengths 795 nm and 762 nm drive a transition from $5S_{1/2}$, $F$=2 to $5D_{3/2}$, $F$=3 [Fig. 1(b)]. A parametric conversion process along a cascade decay channel generates time-ordered photon pairs. We collect herald (776 nm) and probe (780 nm) photons via interference filters into single mode fibers [33–35]. Detecting photons at 776 nm then heralds single photons at 780 nm, which are resonant with the $^{87}$Rb D2 transition. Due to collective effects in the atomic ensemble, the bandwidth of the probe photons is broader than the natural linewidth ($\Gamma_0/2\pi = 6.07$ MHz) of the $5P_{3/2} - 5S_{1/2}$ transition [30, 36]. We employ these effects to tune the bandwidth $\Gamma_\mathrm{p}$ of the probe photons over a range of 6 to 2 $\Gamma_0$ by controlling the number and density of atoms in the cold ensemble via the gradient of the magnetic quadrupole field during the MOT phase.

The probe photons are sent to the single atom setup via a 230 m long optical fiber. To suppress unheralded photons from the FWM setup, an acousto-optic modulator (AOM) acts as a switch between the photon source and the single atom that is opened for 600 ns by a heralding event on detector $\mathrm{D_h}$. Optical and electrical delays are set such that the probe photon passes the AOM in the center of this interval. This AOM also compensates for the 72 MHz shift of the atomic resonance frequency caused by the bias magnetic field and the dipole trap. Probe photons are focused onto the atom by the first aspheric lens. The transmitted probe mode is then collimated again by a second aspheric lens, subsequently coupled into a single-mode fiber, and sent to the forward detector $\mathrm{D_f}$. In previous experiments we determined the spatial overlap of the probe mode with the atomic dipole mode to be $\Lambda \approx 0.033$ [13].

For each bandwidth setting, we obtain a coincidence histogram by sorting the detection times $t_\mathrm{i}$ at $\mathrm{D_f}$ with respect to the heralding event into $\Delta t = 1$ ns wide time bins. Figure 2 shows reference histograms $G_0(t_\mathrm{i})$ with no trapped atoms, normalized to the heralding efficiency $\eta_\mathrm{f} = \sum_i G_0(t_\mathrm{i})$ over the time interval $-10\,\mathrm{ns} \leq t_i \leq 100\,\mathrm{ns}$. The time-ordering of herald and probe photons leads to an asymmetric exponentially decaying profile, from which we extract the corresponding photon bandwidth $\Gamma_\mathrm{p}$ by fitting to Eq. (3) within the range $2\,\mathrm{ns} \leq t_i \leq 100\,\mathrm{ns}$.

When the atom is trapped, we record a corresponding set of probe histograms $G(t_\mathrm{i})$ in a similar way. From this, we can determine the extinction via

$$\epsilon = 1 - \sum_i G(t_\mathrm{i}) \,/\, \sum_i G_0(t_\mathrm{i}) \tag{6}$$

to characterize the photon-atom interaction. Both summations are performed over the time interval $-10\,\mathrm{ns} \leq t_i \leq 100\,\mathrm{ns}$.

## 4. Results

The results of the extinction measurements for bandwidth values between 6 to $2\Gamma_0$ are shown in Fig. 3. Consistent with the model [Eq. (2)], the extinction increases for narrower photon bandwidths. Since our heralded photon source cannot efficiently prepare photons with a bandwidth below $2\Gamma_0$, we simulate photons with $\Gamma_\mathrm{p} \to 0$ by using 100 ms long pulses of laser light with an intensity well below saturation (average number of photons per pulse $\approx$ 1000). The observed extinction of the weak coherent field (Fig. 3, diamond) is larger than the extinction of the heralded photons, but deviates considerably from the model. We attribute this mostly to linewidth

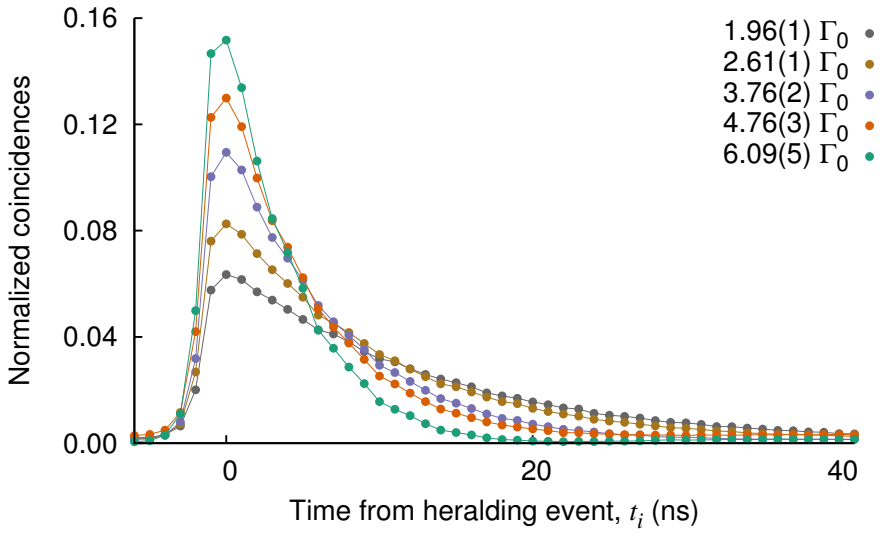


Fig. 2. Coincidence histograms between heralding detector $D_h$ and forward detector $D_f$ for probe photons with five different bandwidths. The bandwidths, shown in the figure legends, are determined by fitting the histograms to Eq. (3). Each histogram is normalized to the heralding efficiency $\eta_f$. Error bars are smaller than symbol size (one standard deviation of propagated Poissonian counting uncertainties). Detection times are offset to account for delays introduced by electrical and optical lines.

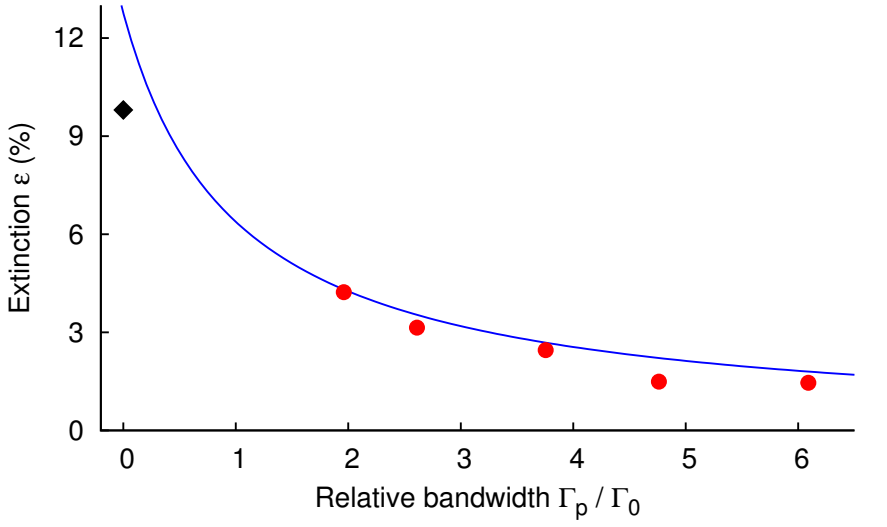


Fig. 3. Extinction $\epsilon$ of probe photons with different bandwidth $\Gamma_p$ (circles). For comparison we include the observed extinction of weak coherent field (diamond). Solid line: Eq. (2) with $\Lambda = 0.033$. Error bars are smaller than symbol size (one standard deviation of propagated Poissonian counting uncertainties).

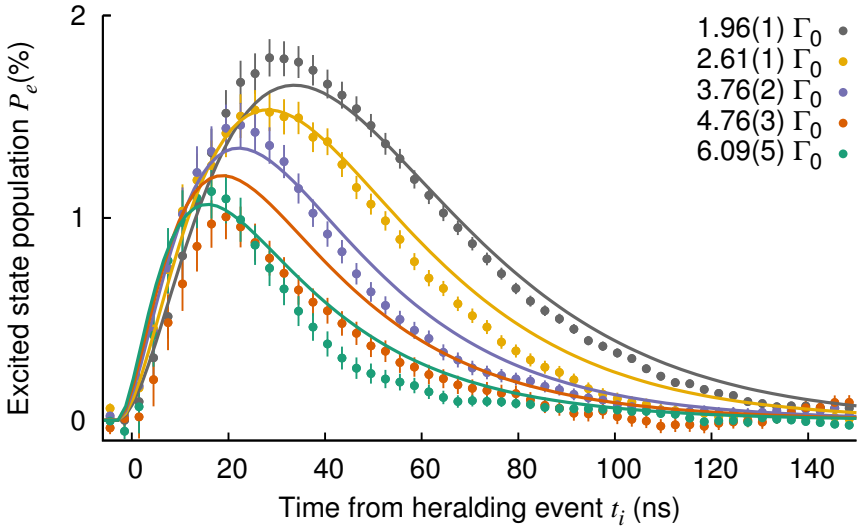


Fig. 4. Temporal evolution of the atomic excited population $P_\mathrm{e}(t)$ obtained from the time-resolved changes in transmission detection rate [see Eq. (7)]. Narrowband photons lead to stronger and longer lasting atomic excitation, in agreement with Eq. (4) (solid lines). Error bars represent one standard deviation of the distributions obtained by a Monte-Carlo method which assumes Poissonian statistics for the detection rates.

broadening of the atomic transition: when tuning the frequency of the coherent probe field across the atomic resonance, we observe a linewidth of $2\pi \cdot 10.6(6)\,\mathrm{MHz} = 1.7(1)\Gamma_0$ in the transmission spectrum. This broadening can be caused by intensity fluctuations of the dipole trap field, the atomic motion of the atom, and the probe laser linewidth [37]. The heralded photons from FWM have a larger bandwidth, so their scattering probability is less susceptible to this broadening of the atomic transition.

Aside from the scattering probability, we also determine the temporal evolution of the atomic excited population $P_\mathrm{e}(t)$ during the scattering process. Any change of the forward detection rate $\delta\,(t_\mathrm{i}) = (G_0(t_\mathrm{i}) - G(t_\mathrm{i}))\,/(\eta_\mathrm{f}\Delta t)$ is directly related to a change $\dot{P}_\mathrm{e}(t)$ of the atomic population [13] via the rate equation

$$\dot{P}_\mathrm{e}(t) = \delta(t) - (1-\Lambda)\Gamma_0 P_\mathrm{e}(t)\,. \tag{7}$$

Thus, $P_\mathrm{e}(t)$ can be obtained by integrating Eq. (7) with a relatively low experimental uncertainty. Figure 4 shows the evolution of the resulting $P_\mathrm{e}(t)$, agreeing very well with Eq. (4) (solid lines) for narrowband photons, but exhibit a stronger deviation from the model as the bandwidth is increased. This deviation is likely due to the imperfect photon profiles on the sharp rising edge (Fig. 2) compared to the ideal asymmetric exponentially decaying profile.

The peak excitation probability $P_\mathrm{e,max}$ for each bandwidth in Fig. 4 is shown in Figure 5, and is in good agreement with Eq. (5). Comparing results for narrowband ($\Gamma_\mathrm{p} = 1.96(1)\Gamma_0$) and broadband ($\Gamma_\mathrm{p} = 6.09(5)\Gamma_0$) photons, we observe an increase in the peak excitation by a factor 1.5(2). This relative increase is smaller than the relative increase by a factor of 2.6(4) of the extinction between these two bandwidths, i.e. the atomic peak excitation has a weaker dependence on the photon bandwidth than the scattering probability over our accessible bandwidth range.

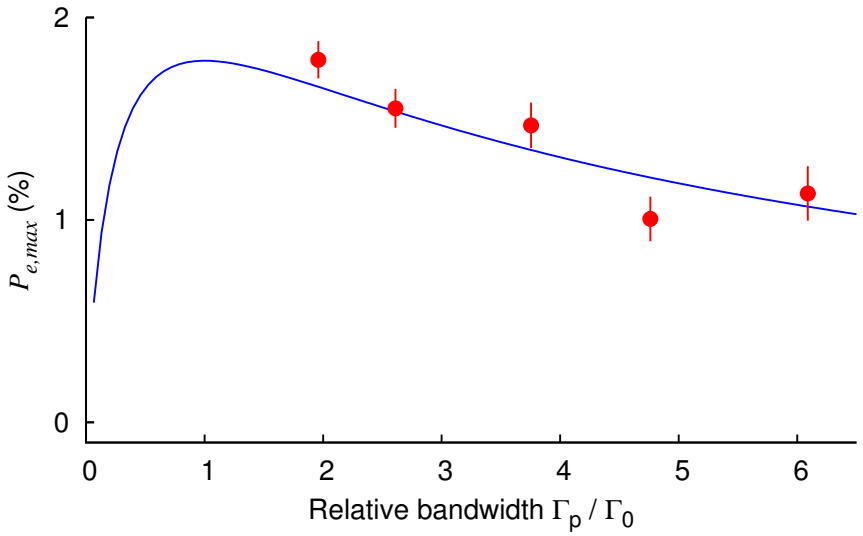


Fig. 5. Atomic peak excitation $P_{\mathrm{e,\,max}}(t)$, extracted from the experimental $P_{\mathrm{e}}(t)$ curves shown in Fig. 4. Solid line: Eq. (5).

## 5. Discussion and summary

While often a semiclassical description of light-atom interaction can explain observations with sufficient accuracy, it is well known that the photon statistics of the incident light can affect the atomic excitation dynamics [18, 25, 38, 39]. Full quantum models of the light-matter interaction predict different scattering probabilities for single photons compared to coherent fields with equal bandwidth and a mean photon number of one [18, 25]. As (hybrid) quantum networks in an information processing scenario are likely to operate by exchanging single photons, testing light-matter interfaces with single photons – as opposed to weak coherent fields – becomes important. For the experimental parameters in the work presented here ($\Lambda = 0.033$, $\Gamma_{\mathrm{p}} = 2\Gamma_0$), the expected difference in scattering probability is only 0.05%, and thus within our experimental uncertainties. However, a slight improvement of experimental parameters should make the difference in scattering resolvable, assuming similar experimental uncertainties. For $\Lambda = 0.1$ and $\Gamma_{\mathrm{p}} = \Gamma_0$, quite within experimentally reachable range [40], we expect $\epsilon = 18.0\%$ for single photon excitation, but $\epsilon = 17.1\%$ for a coherent field.

In summary, we find that the role of the photon bandwidth in the scattering process with a single atom is well described by a relatively simple excitation model with a fully quantized field description [25]. Tuning the photon bandwidth from 6 to 2 $\Gamma_0$, we observe an increase in the scattering probability as well as in the atomic peak excitation. Notably, the relative increase in the scattering probability is larger than in the atomic peak excitation.

## Funding

Ministry of Education in Singapore (AcRF Tier 1); National Research Foundation, Prime Minister's office (partly under grant No. NRF-CRP12-2013-03); M. Steiner acknowledges support by the Lee Kuan Yew Postdoctoral Fellowship.